arXiv:hep-ex/0511036v2 16 Nov 2005

SINGLE SPIN ASYMMETRY OF CHARGED HADRON PRODUCTION BY 40 GEV/C POLARIZED PROTONS

V.V. Abramov[1]†, P.I. Goncharov[1], A.Yu. Kalinin[1], A.V. Khmelnikov[1], A.V. Korablev[1],
Yu.P. Korneev[1], A.V. Kostritsky[1], A.N. Krinitsyn[1], V.I. Kryshkin[1], A.A. Markov[1],
V.V. Talov[1], L.K. Turchanovich[1], A.A. Volkov[1]

(1) *Institute for High Energy Physics, Protvino, Moscow region, Russia*
† *E-mail: Victor.Abramov@ihep.ru*

Abstract

The single spin asymmetry for charge hadron production off nuclei (C, Cu) has been measured using 40 GeV/c polarized proton beam. The measurements were carried out using FODS-2 experimental setup at IHEP. The data are presented in the central region and the forward region with respect to the incident protons.

1 Introduction

The single spin asymmetries (SSA) in hadron-hadron interactions are much larger than expected from the naive pertubative QCD [1]. Also, its dependence on kinematic variables and hadron type is far from the complete understanding. The existing data are measured in a limited range of c.m. production angles, transverse momenta and energies. The previous measurements of SSA have shown that its absolute value is rising with the increase of p_T and x_F for beam energies above 20 GeV [2],[3]. There were no measurements so far of the single spin asymmetries of the charged hadron production in the energy range between 22 and 200 GeV. We have measured the single-spin asymmetry A_N of the inclusive charged pion, kaon, proton and antiproton production cross sections at high p_T and high x_F regions for a 40 GeV/c polarized proton beam incident on nuclei (C, Cu), where A_N is defined as

$$A_N = \frac{1}{P_B \cdot cos\phi} \cdot \frac{N\uparrow - N\downarrow}{N\uparrow + N\downarrow}, \tag{1}$$

where P_B is the beam polarization, ϕ is the azimuthal angle of the production plane, $N\uparrow$ and $N\downarrow$ are event rates for the beam spin up and down respectively. The measurements were carried out at IHEP, Protvino in 2003. The preliminary results in the central region were reported elsewhere [4]. The measurements of A_N in the central region using hydrogen target revealed a sizable asymmetry for π^+ and K^+ production [5].

2 Polarized beam and experimental setup

The polarized protons are produced by the parity - nonconserving Λ decays [4],[5]. The up or down beam transverse polarization is achieved by the selection of decay protons with angles near 90° in the Λ rest frame by a movable collimator. At the end of the beam line two magnets correct the vertical beam position on the spectrometer target for the two beam polarizations. The intensity of the 40 GeV/c momentum polarized beam on the spectrometer target is 3×10^7 ppp, $\Delta p/p = \pm 4.5\%$, the transverse polarization is

39^{+1}_{-3} %, and the polarization direction is changed each 18 min during 30 s. The beam intensity and the position are measured by the ionization chambers and the scintillation hodoscopes.

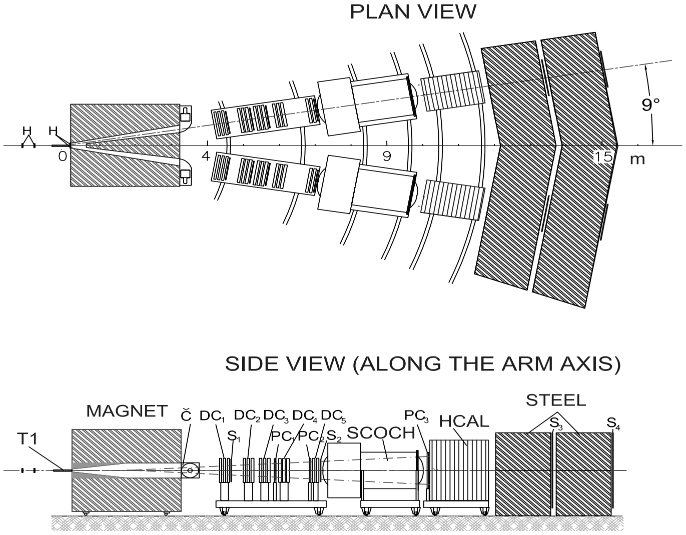

Figure 1: Schematic of experimental layout FODS-2.

The measurements were carried out with the FODS-2 [4],[5] spectrometer (Fig. 1). It consists of an analyzing magnet, the drift chambers, the Cherenkov radiation spectrometer (SCOCH) for the particle identification ($\pi^{\pm}$, $K^{\pm}$, p and $\bar{p}$), the scintillation counters, and the hadron calorimeters to trigger on the high energy hadrons. Inside the magnet there is also a beam dump made of tungsten and copper. There are two arms which can be rotated around the target center situated in front of the magnet to change the secondary particle angle.

There are two threshold Cherenkov counters using air at the atmospheric pressure inserted in the magnet which are used for further improvement of particle identification.

3 Measurements

The measurements of A_N in the range $-0.15 \leq x_F \leq 0.2$ and $0.5 \leq p_T \leq 4$ GeV/c are carried out with the symmetrical arm positions at angles of ± 160 mrad (mean c.m. angle $\theta_{cm} = \pm\ 86^o$). The results for the two arms and the different values of the magnetic field B in the spectrometer are averaged, which partially cancels systematical uncertainties connected with the variation of the beam position in the vertical direction, the intensity monitor and the apparatus drift. Another set of measurements is carried out with the arms, rotated by 70 mrad (the left arm is at $\theta_{cm} = 48^o$ with $0.05 \leq x_F \leq 0.7$ and $0.5 \leq p_T \leq 2.5$ GeV/c , and the right arm is at $\theta_{cm} = 105^o$ with $-0.25 \leq x_F \leq -0.05$ and $0.7 \leq p_T \leq 3$ GeV/c). Both polarities of magnetic field B in the spectrometer magnet are used for data taking to reduce systematic uncertainties. In addition, two values of the magnetic field (B and B/2) are used to extend the momentum range of the data.

4 Data processing

The reconstructed trajectory of a particle downstream the spectrometer magnet and beam coordinates from the beam hodoscopes are used to determine its momentum, production angles and vertex Z-coordinate. After all cuts are applied, the remaining events are identified in the SCOCH and threshold cherenkov counters. The integrated beam flux is measured by the ionization chamber and is used to calculate normalized particle rates ($N\uparrow$ and $N\downarrow$) for two signs of the beam polarization. The beam coordinates, measured by the X and Y hodoscope planes, are used to estimate the mean beam position (X_B and Y_B) during a spill, separately for "UP" and "Down" polarization signs. It was found that the mean beam coordinates, averaged over a group of runs with similar conditions, can differ for "UP" and "Down" beam polarizations up to ±0.5 mm. Since the normalized rates $N\uparrow$ and $N\downarrow$ depend on the beam position, the false asymmetry can be added to the analyzing power A_N. Cuts on beam coordinates are imposed to level the X_B and Y_B for "UP" and "Down" polarization sign with 4 μm accuracy to avoid the false asymmetry. The other sources of systematic uncertainties, remaining after the above cuts are applied, contribute up to 4% to the systematic error ϵ, which is estimated from run to run A_N variation. The ϵ is added in the quadrature to the statistical error at each data point.

5 Single spin asymmetries

The dependence of A_N on transverse momentum (p_T) for $\pi^\pm$, K$^\pm$, p and $\bar{\text{p}}$ production on C and Cu targets and at two c.m. angles ($\approx 48^o$ and $\approx 85^o$) are shown in Figs. 2 - 7. The significant value of A_N is seen in π^+, π^-, K^+ and proton production at $\theta_{cm} \approx 48^o$ on both targets. The A_N at $\theta_{cm} \approx 85^o$ is approximately two times smaller in π^+ and K^+ production and reveals a breakdown at $p_T \approx 2.5$ GeV/c in its p_T dependence, which could indicate a transition to the predicted pQCD regime [1]. The A_N for K^- and $\bar{p}$ production is consistent with zero for both targets and all c.m. angles, as expected due to small sea quark polarization. The proton data at $\theta_{cm} \approx 48^o$ reveal an oscillation of A_N

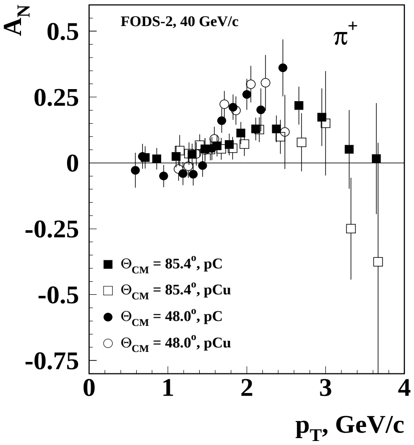

Figure 2: A_N dependence on p_T for p$\uparrow$ +C(Cu) $\rightarrow \pi^+ +$ X.

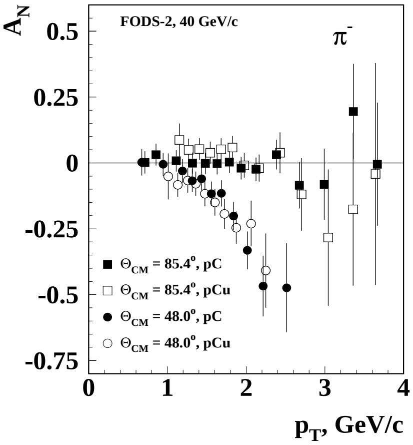

Figure 3: A_N dependence on p_T for p$\uparrow$ +C(Cu) $\rightarrow \pi^- +$ X.

with minimum at 1.3 GeV/c and maximum near 2.2 GeV/c. The SSA at $\theta_{cm} \approx 105^o$

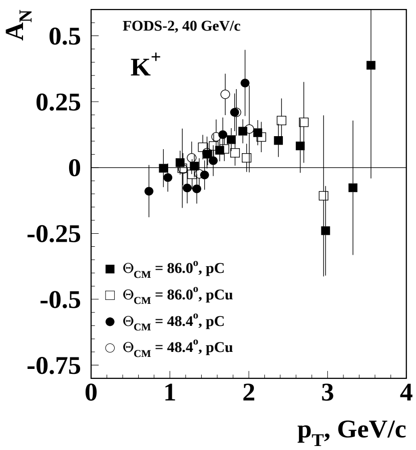

Figure 4: A_N dependence on p_T for p$\uparrow$ +C(Cu) $\rightarrow$ K$^+$ + X.

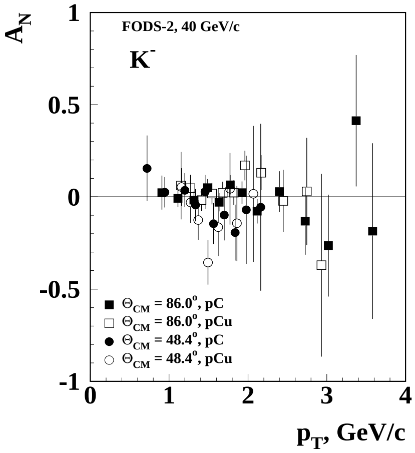

Figure 5: A_N dependence on p_T for p$\uparrow$ +C(Cu) $\rightarrow$ K$^-$ + X.

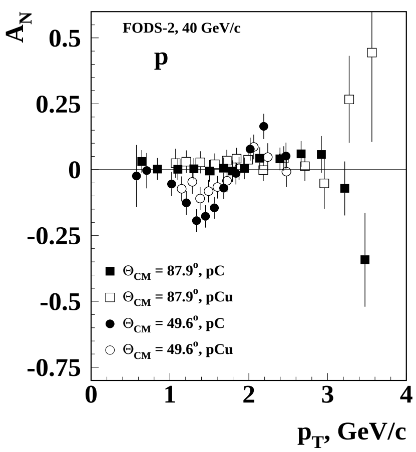

Figure 6: A_N dependence on p_T for p$\uparrow$ +C(Cu) $\rightarrow$ p + X.

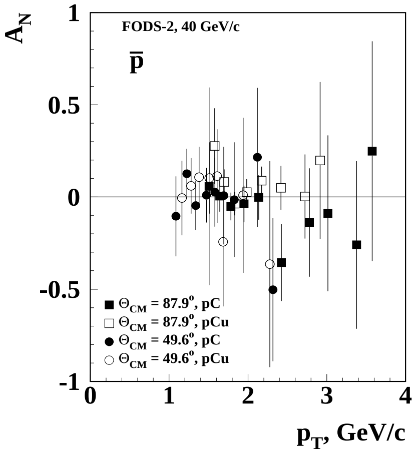

Figure 7: A_N dependence on p_T for p$\uparrow$ +C(Cu) $\rightarrow$ $\bar{\rm p}$ + X.

are shown in Figs. 8 and 9 for π^+ and π^-, respectively. For all charged hadrons the SSA is close to zero at θ_{cm} near 105^o. No significant A-dependence is observed in the above data.

Comparison of FODS-2 results with the data, measured at 22 GeV/c [3] and at 200 GeV/c [2], is shown in Figs. 8 - 9 as a function of a scaling variable $X_S = (X_R + X_F)/2 - X_0$, where $X_0 = 0.075N_Q + 2N_QM_Q(1+\cos\theta_{cm})/\sqrt{s}$ takes into account the constituent quark mass $M_Q = 0.3$ GeV/c^2 and the number N_Q of valence quarks in the observed hadron. For all three energies the π^+ SSA in the forward region is described well by a single function of X_S. The π^- and proton SSA agree with E925 data for $p_T \geq 0.6$ GeV/c [4]. References to other examples of scaling SSA behavior can be found in Ref. [4].

In conclusion, the SSA are measured on C and Cu targets for $\pi^\pm$, $K^\pm$, $\bar{p}$ and proton production at mean c.m. angles 48^o, 86^o and 105^o. The decrease of SSA above 2.5 GeV/c for π^+, K^+ and protons can indicate a transition to the pQCD regime, where A_N tends to zero. No significant A-dependence is observed for the SSA. The SSA for K^- and $\bar{p}$ are consistent with zero, as expected due to the small sea quark polarization. The scaling behavior of SSA is seen for $\theta_{cm} \leq 50^o$ and $p_T \geq 0.6$ GeV/c. The SSA is close to zero for $\theta_{cm} \approx 105^o$.

We are grateful to the IHEP staff for their assistance with setting up the experiment and the IHEP directorate for their support.

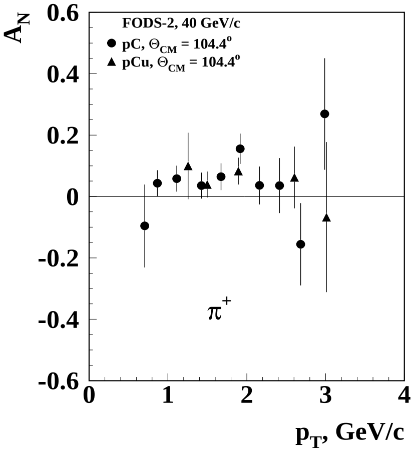

Figure 8: A_N vs p_T at 104.4^o.

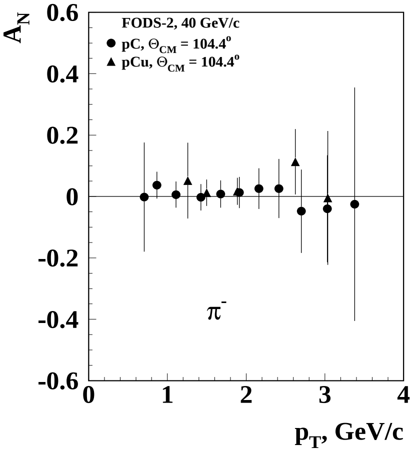

Figure 9: A_N vs p_T at 104.4^o.

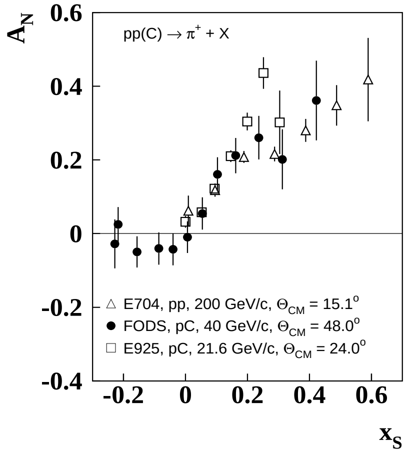

Figure 10: A_N vs X_S for π^+ production at 22, 40, and 200 GeV.

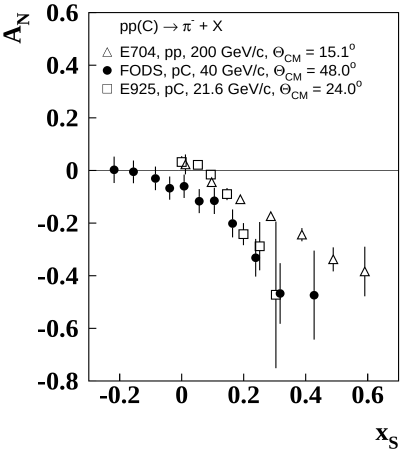

Figure 11: A_N vs X_S for π^- production at 22, 40, and 200 GeV.

References

[1] G. Kane, J. Pumplin, and W. Repko, *Phys. Rev. Lett.* **41**, 1689 (1978).

[2] D.L. Adams *et al.*, *Phys. Lett.* **B264**, 462 (1991).

[3] K. Krueger *et al.*, *Phys. Lett.* **B459**, 412 (1999).

[4] V.V. Abramov, *Phys. Atom. Nucl.* **68**, 385 (2005).

[5] V.V. Abramov, A.S. Dyshkant, V.N. Evdokomov *et al.*, *Nucl. Phys.* **B492**, 3 (1997).